

A Dynamical Systems Analysis of Axisymmetric Accretion in a Schwarzschild Black Hole

Shamreen Iram^{*1}

¹Indian Institute of Technology, Kanpur, Uttar Pradesh-208016, India

February 23, 2022

Abstract

Stationary, inviscid, axisymmetric, rotating, transonic accretion flow has been studied in a general relativistic framework, in the Schwarzschild metric; for three different flow geometries - under both polytropic and isothermal conditions. The equilibrium points of the underlying fluid system have been located and an eigenvalue based linear dynamical systems analysis of these critical points has been carried out, to obtain a taxonomic scheme of the critical points. It has hence been shown that only saddle and centre type points can arise for real, physical transonic flow.

1 Introduction

Spectroscopy, traditionally the sturdiest observational tool in astrophysics, has not been of much help in garnering direct observational evidence, when it comes to astrophysical black holes. The obscuring presence of the event horizon makes any such 'visibility' nigh impossible. One must then take recourse to the fact that an astrophysical black hole, being a strongly gravitating body, should leave several gravitational signatures upon its surrounding space-time, which could be used as indirect evidence of its presence.

A few important such phenomenon spurring great interest in current research include the possibility of remarkable 'lensing' effects that could be produced by the deep gravitational potential wells around isolated black holes. Of specific motivational relevance to this study are the radiative emissions that could be caused by infalling matter accreting on to a black hole when rest mass undergoes conversion to radiation. An accreting black hole may be detected this way [1].

An astrophysical black hole in a matter rich environment or with access to a matter source, will accrete matter towards itself, and in the process an accretion disc may be formed. In the context of thermal, and thus sonic behaviour, the accreting matter when starting out sufficiently far from the accretor (i.e black hole, here) may be assumed to be moving slow or subsonically. It speeds up along the way as it spirals in inwards. The black hole inner boundary condition implies perforce that the flow must be supersonic when it crosses the event horizon. Thus, unlike accretion by any regular strongly gravitating body, black hole accretion must necessarily be transonic in nature. The transition from subsonic to supersonic flow can proceed either smoothly and continuously [2], or via discontinuous[4, 3], violently dissipative shock transitions[3].

This study has been carried out for stationary, inviscid, hydrodynamic accretion, in axisymmetric configurations of three different flow disc geometries- namely, constant height disc geometry, conical disc geometry, and a disc in vertical equilibrium. Thermodynamic conditions pertaining to different equations of state have been considered, varying from a range of polytropic conditions,

^{*}samreen654@gmail.com

ending with pure isothermal. Now, real, physical transonic solutions connecting our zones of interest (the event horizon with the source of accreting material, effectively infinity) may be formally obtained as critical solutions on the phase plane of the flow- spanning flow velocity and radial distance. By virtue of simultaneously satisfying the conditions of physicality and transonicity, these solutions must necessarily be associated with saddle type critical points- the only kind that will allow the solution to double up and pass through itself.

In this paper, the fundamental, governing non-linear equations for stationary, inviscid, hydrodynamic, rotating axisymmetric accretion flow in the Schwarzschild metric have been mapped onto a first order, autonomous dynamical system [5]. A full and comprehensive global picture of the phase space topology will involve taking recourse to complete numerical integration of the system of non-linear coupled differential flow equations. Here, an alternative quasi-analytical approach has been presented which employs further dynamical systems based techniques to gain further insight into the nature of these critical points. First, the critical points of the flow have been located computationally and the parameter space spanned by the solutions identified. Thereafter, the autonomous system has been subsequently linearized about these critical points and a complete, rigorous and equivalent, eigenvalue based classification formalism has been developed to identify the nature of the critical points. This has been carried out for three different prior mentioned geometric flow configurations, and various equations of state. It has hence been shown that the only type of critical points possible on the flow trajectory are of saddle or centre type.

The treatment and procedure presented in this paper has been employed in earlier works, and follows and builds up from them. One work has carried out the study for a pseudo-Newtonian potential[6, 7]. While another has investigated the procedure in the Kerr metric, for the case of polytropic flow in a disc in vertical equilibrium, and examined the result in the Schwarzschild limit[3]. This work extends it to other flow geometries, and all possible equations of state (namely a range of polytropic to isothermal), in the Schwarzschild metric.

2 Background Configuration of the Flow and Critical Points

The subject of this treatment is on self-gravitating axis-symmetric, inviscid hydrodynamic accretion onto a non-rotating, i.e., Schwarzschild black hole, in the low angular momentum regime.

Such slowly rotating spiraling flows are not merely theoretical abstractions, as has been stated in previous literature [8, 7]. Several astrophysical systems like detached binary systems fed by accretion from OB stellar winds [9, 10], semi-detached low magnetic binaries[11], and supermassive black holes fed by accretion from slowly rotating central stellar clusters [12, 13] provide prime examples.

In such a background configuration, the fundamental governing equations of the flow have been first set up, under polytropic thermodynamic conditions, followed by accretion under isothermal conditions.

2.1 Polytropic Accretion

Bernoulli's equation can be expressed analogously in its relativistic form [14, 15, 16, 3]

$$\varepsilon = hv_t \tag{1}$$

where ε is the specific flow energy, h is the specific enthalpy of the system and v_t is the temporal component of the 4-velocity.

The equation of state is taken to be of the form

$$P = k\rho^\gamma \quad (2)$$

where γ is the usual polytropic index, the ratio of the specific heats at constant pressure C_p and at constant volume C_v . k provides a measure of the specific entropy of the accreting fluid, at constant entropy [8] .

The specific enthalpy is of the form

$$h = \frac{P + \epsilon}{\rho} \quad (3)$$

where energy density ϵ is a function of the rest mass density and internal energy, and is defined as

$$\epsilon = \rho + \frac{P}{\gamma - 1} \quad (4)$$

Plugging in the above defined equation in the equation of state, the definition for advective sound speed becomes:

$$c_s^2 = \left. \frac{\partial P}{\partial \epsilon} \right|_{h=const.} \quad (5)$$

Now, at constant entropy, the enthalpy can be expressed as

$$h = \frac{\partial \epsilon}{\partial \rho} \quad (6)$$

This defines the expression for h as

$$h = \frac{\gamma - 1}{\gamma - (1 + c_s^2)} \quad (7)$$

The final explicit expression for conserved ε is given as [8]

$$\varepsilon = -\frac{\gamma - 1}{\gamma - (1 + c_s^2)} \sqrt{\frac{1 - 2/r}{\left[1 - \frac{\lambda^2}{r^2}(1 - 2/r)\right](1 - u^2)}} \quad (8)$$

The transformation

$$\dot{\Xi} = \dot{M} K^{1/(\gamma-1)} \gamma^{1/(\gamma-1)} \quad (9)$$

where $\dot{\Xi}$ is the entropy accretion rate, while K gives a measure of the specific entropy of the infalling accreting matter, has been used to locate and separate out the accretion and the wind zones, in the multi-critical parts of the parameter space.

2.1.1 Constant Height Model

H plays a trivial role in this model, which shows translational symmetry along its vertical axis. The conserved mass accretion rate is [8]:

$$\dot{M} = 2\pi\rho u \sqrt{\frac{1-2/r}{1-u^2}} r H \quad (10)$$

which defines

$$\dot{\Xi} = 2\pi u \sqrt{\frac{1-2/r}{1-u^2}} r c_s^{\frac{2}{\gamma-1}} \left[\frac{\gamma-1}{\gamma-(1+c_s^2)} \right]^{\frac{1}{\gamma-1}} H \quad (11)$$

Differentiating the two conserved quantities ε and $\dot{\Xi}$ and combining the two obtained relations between $\frac{dc_s}{dr}$ and $\frac{du}{dr}$ gives the following final spatial value of change of advective velocity [8]

$$\frac{du}{dr} = \frac{c_s^2 \left[\frac{1}{r} + \frac{1}{r^2(1-2/r)} \right] - f_2(r, \lambda)}{(1-c_s^2) \frac{u}{1-u^2} - \frac{c_s^2}{u}} = \frac{N}{D} \quad (12)$$

where

$$f_2 = -\frac{\lambda^2}{r^3} \left[\frac{1-3/r}{1-\frac{\lambda^2}{r^2}(1-2/r)} \right] + \frac{1}{r^2(1-2/r)} \quad (13)$$

The critical point conditions then become fixed on the u-r phase plane as (setting N and D to 0)

$$[u = c_s]_{r_c} \quad [c_s]_{r_c} = \sqrt{\frac{f_2}{\frac{1}{r_c} + \frac{1}{r_c^2(1-2/r_c)}}} \quad (14)$$

$[\varepsilon, \lambda, \gamma]$ and relation (14) have now been used to numerically locate the critical points of the flow, and demarcate the mono and the multi-linear zones in parameter space.

The astrophysically relevant domain for these numerical computations are $[1 \leq \varepsilon \leq 2]$, $[0 \leq \lambda \leq 4]$, $[\frac{4}{3} \leq \gamma \leq \frac{5}{3}]$

2.1.2 Flow in Conical Equilibrium

The height is now taken to be quasi-spherical, and mass accretion and entropy accretion rates are appropriately modified to : [8]

$$\dot{M} = \Lambda \rho u \sqrt{\frac{1-2/r}{1-u^2}} r^2 \quad (15)$$

$$\dot{\Xi} = \Lambda u \sqrt{\frac{1-2/r}{1-u^2}} r^2 c_s^{\frac{2}{\gamma-1}} \left[\frac{\gamma-1}{\gamma-(1+c_s^2)} \right]^{\frac{1}{\gamma-1}} \quad (16)$$

where Λ is a constant factor determining the radial shape of the flow. Proceeding as above,

$$\frac{du}{dr} = -\frac{c_s^2 \left[\frac{2}{r} + \frac{1}{r^2(1-2/r)} \right] - f_2}{\frac{u}{1-u^2}(c_s^2 - 1) - \frac{c_s^2}{u}} \quad (17)$$

giving the critical point conditions :

$$[u = c_s]_{r_c} \quad [c_s]_{r_c} = \sqrt{\frac{f_2}{\frac{2}{r_c} + \frac{1}{r_c^2(1-2/r_c)}}} \quad (18)$$

2.1.3 Flow in Vertical Equilibrium

The disc height for flow in the hydrostatic equilibrium in vertical direction can be taken to be [16]

$$H(r) = \frac{r^2 c_s}{\lambda} \sqrt{\frac{2(1-u^2)[1 - \frac{\lambda^2}{r^2}(1-2/r)](\gamma-1)}{\gamma(1-2/r)[\gamma - (1+c_s^2)]}} \quad (19)$$

Mass and entropy accretion become [8]

$$\dot{M} = 4\pi\rho \sqrt{\frac{u(1-2/r)}{1-u^2}} \frac{r^4 c_s}{\lambda} \sqrt{\frac{2(1-u^2)[1 - \frac{\lambda^2}{r^2}(1-2/r)](\gamma-1)}{\gamma(1-2/r)[\gamma - (1+s^2)]}} \quad (20)$$

$$\dot{\Xi} = \sqrt{\frac{2}{\gamma}} \left[\frac{\gamma-1}{\gamma - (1+c_s^2)} \right]^{\frac{\gamma+1}{2(\gamma-1)}} \frac{c_s^{\frac{\gamma-1}{\gamma+1}}}{\lambda} \sqrt{1 - \frac{\lambda^2}{r^2}(1-2/r)} (4\pi u r^3) \quad (21)$$

giving [8]

$$\frac{du}{dr} = \frac{\frac{2c_s^2}{\gamma+1} f_1(r, \lambda) - f_2(r, \lambda)}{\frac{u}{1-u^2} - \frac{2c_s^2}{u(\gamma+1)}} \quad (22)$$

where $f_1(r, \lambda) = \frac{3}{r} + \frac{\lambda^2}{r^3} \left[\frac{1-3/r}{1 - \frac{\lambda^2}{r^2}(1-2/r)} \right]$

The critical point conditions come out to be

$$u_c = \sqrt{\frac{1}{1 + (\frac{\gamma+1}{2}) \frac{1}{c_{sc}^2}}} = \sqrt{\frac{f_2}{f_1 + f_2}} \quad (23)$$

Therefore, it can be seen that the critical and the sonic points are not isomorphic.

2.2 Isothermal Accretion

For isothermal accretion flow, the equation of state considered is of the form

$$p = \rho c_s^2 = \frac{R}{\mu} \rho T = \frac{\rho k_B}{\mu m_H} T \quad (24)$$

where R , k_B , μ , m_H and T are the universal gas constant, the Boltzmann constant, the reduced mass, mass of the hydrogen atom and the isothermal flow temperature. It is evident from above that the isothermal sound speed c_s is thus a position independent global flow constant. Under such condition, the static general relativistic fluid equations deliver the following first integral of motion independent of disc geometry [8]

$$\xi = \frac{r^2(r-2)}{[r^3 - (r-2)\lambda^2](1-u^2)} \rho^{2c_s^2} \quad (25)$$

This is the analogous conserved quantity for isothermal flow corresponding to conserved energy ε for polytropic accretion.

For this case, the sound speed being a constant, ξ has been used to separate out the accretion and wind zones after locating the multi-critical parts of parameter space.

2.2.1 Constant Height Model

The mass accretion rate and ξ together give [8]

$$\frac{du}{dr} = \frac{[2r^3 - 2(r-2)^2\lambda^2 + (1-r)(2r^3 + 4\lambda^2 - 2r\lambda^2)c_s^2]u(u^2 - 1)}{r(2-r)[-2r^3 - 4\lambda^2 + 2r\lambda^2](u^2 - c_s^2)} \quad (26)$$

delivering the critical point conditions as

$$[u = c_s]_{r_c} \quad c_s^2 = \left[\frac{-r^3 + (r-2)^2\lambda^2}{r^3 - r^4 + (r-2)(r-1)\lambda^2} \right]_{r_c} \quad (27)$$

Using the value of c_s^2 from the Clayperon-Mendeleev equation as input above, taking T and λ as parameters, the critical points have now been located. Further, from \dot{M} (which is a constant), plugging in ρ back into ξ , the accretion and wind zones have been separated out.

2.2.2 Disc in Conical Equilibrium

The space gradient of advective velocity comes out to be [8]:

$$\frac{du}{dr} = \frac{[2r^3 - 2(r-2)^2\lambda^2 + (3-2r)(2r^3 + 4\lambda^2 - 2r\lambda^2)c_s^2]u(u^2 - 1)}{r(2-r)[-2r^3 - 4\lambda^2 + 2r\lambda^2](u^2 - c_s^2)} \quad (28)$$

The critical point conditions are fixed as

$$[u = c_s]_{r_c} \quad c_s^2 = \left[\frac{-r^3 + (r-2)^2\lambda^2}{3r^3 - 2r^4 + 6\lambda^2 - 7r\lambda^2 + 2r^2\lambda^2} \right]_{r_c} \quad (29)$$

2.2.3 Flow in Vertical Equilibrium

Unlike the other two models, taking constant sound speed, the disc height for flow in this geometric configuration modifies to [8]:

$$H(r)^{iso} = rc_s \frac{\sqrt{2[r^3 - (r-2)\lambda^2](1-u^2)}}{\lambda\sqrt{r-2}} \quad (30)$$

giving mass accretion rate

$$\dot{M} = 4\pi\rho \frac{r^2 uc_s}{\lambda} \sqrt{2[r^3 - (r-2)\lambda^2]} \quad (31)$$

and [8]:

$$\frac{du}{dr} = \frac{2[r^3 - (r-2)^2\lambda^2 + (2-r)(4r^3 + 5\lambda^2 - 3r\lambda^2)c_s^2]u(u^2 - 1)}{r(r-2)[-2r^3 - 4\lambda^2 + 2r\lambda^2][c_s^2 - (1+c_s^2)u^2]} \quad (32)$$

They give the following critical pair conditions [8]:

$$\left[u^2 = \frac{c_s^2}{1+c_s^2} = \frac{-r^3 + (r-2)^2\lambda^2}{8r^3 - 4r^4 + 10\lambda^2 - 11r\lambda^2 + 3r^2\lambda^2} \right]_{r_c} \quad (33)$$

As is evident, unlike the cases of constant height and disc in conical equilibrium, the sonic points and critical points do not coincide in this case and are not isomorphic. Thus for general relativistic isothermal flow in the Schwarzschild metric, the Mach number at the critical surface is not 1. It is interesting to note at this point that for isothermal axis-symmetric accretion in Newtonian [17] and pseudo-Schwarzschild [7] potentials, however, for the case of the disc in vertical equilibrium too, the sonic points had coincided with the critical points.

3 Nature of the Fixed Points : A Dynamical Systems Study

To carry out a dynamical systems study of the fixed points of the flow, the equations for space gradient of advective velocity for the stationary, axis-symmetric rotational flow in the Schwarzschild metric have been first appropriately parametrised and decomposed into an equivalent autonomous first-order dynamical system, in the independent parameter τ [5].

It must be noted here that the equations have now been taken in the $u^2 - r$ plane, to remove any directionality dependence.

3.1 Polytropic Accretion

The following linear perturbation scheme has been applied about the critical point :

$$\begin{aligned} u^2 &= u_c^2 + \delta u^2 \\ c_s^2 &= c_{sc}^2 + \delta c_s^2 \\ r &= r_c + \delta r \end{aligned}$$

Now, the conserved energy equation for polytropic accretion is [8]

$$\varepsilon = -\frac{(\gamma - 1)}{(\gamma - 1 - c_s^2)} \sqrt{\frac{1 - 2/r}{[1 - \frac{\lambda^2}{r^2}(1 - 2/r)](1 - u^2)}} \quad (34)$$

Taking logarithmic differentials delivers the following expression for variation of sound speed

$$\delta c_s^2 = -[\gamma - 1 - c_s^2][p\delta r + q\delta u^2] \quad (35)$$

where the quantities p and q have been defined as

$$p = \frac{1}{r_c(r_c - 2)} - \frac{1}{1 - \frac{\lambda^2}{r_c^2}(1 - 2/r_c)} \left(\frac{\lambda^2}{r_c^3} - \frac{3\lambda^2}{r_c^4} \right) \quad (36)$$

$$q = \frac{1}{2(1 - u_c^2)} \quad (37)$$

3.1.1 Constant Height

From before, the equation for space gradient of advective velocity is [8]

$$\frac{du}{dr} = \frac{c_s^2 \left[\frac{1}{r} + \frac{1}{r^2(1-2/r)} \right] - f_2(r, \lambda)}{(1 - c_s^2) \left(\frac{u}{1-u^2} \right) - \frac{c_s^2}{u}} \quad (38)$$

Going over to the $u^2 - r$ plane and decomposing into a set of parametrised autonomous dynamical equations :

$$\frac{du^2}{d\tau} = 2c_s^2 f_1(r) - 2f_2(r, \lambda) \quad (39)$$

$$\frac{dr}{d\tau} = \frac{1 - c_s^2}{1 - u^2} - \frac{c_s^2}{u^2} \quad (40)$$

where $f_1(r)$ has been defined as $f_1(r) = \frac{1}{r} + \frac{1}{r^2(1-2/r)}$

As before, the critical point conditions corresponding to standing equilibrium points of the system come out to be

$$[u = c_s]_{r_c} \quad c_s = \sqrt{\frac{f_2}{\frac{1}{r_c} + \frac{1}{r_c^2(1-2/r_c)}}} \quad (41)$$

Now perturbing the system linearly about its critical points and applying the critical point conditions, gives the following coupled linear dynamical system :

$$\frac{d(\delta u^2)}{d\tau} = -2f_1q(\gamma - 1 - c_{sc}^2)\delta u^2 + [2c_{sc}^2f'_1 - 2f'_2 - 2f_1p(\gamma - 1 - c_{sc}^2)]\delta r \quad (42)$$

$$\frac{d(\delta r)}{d\tau} = [(\gamma - 1 - c_{sc}^2)q + 1] \left[\frac{1}{(1 - u_c^2)} + \frac{1}{u_c^2} \right] \delta u^2 + (\gamma - 1 - c_{sc}^2) \left[\frac{1}{(1 - u_c^2)} + \frac{1}{u_c^2} \right] p \delta r \quad (43)$$

For exponentially growing solution with eigenvalues Ω , of the kind $\delta u^2 \sim \exp(\Omega\tau)$ and $\delta r \sim \exp(\Omega\tau)$, the stability matrix of the above autonomous system gives eigenvalues

$$\Omega^2 = \frac{2}{u_c^2(u_c^2 - 1)} [f_1p(1 + c_{sc}^2 - \gamma) + (f'_2 - c_{sc}^2f'_1)\{q(1 + c_{sc}^2 - \gamma) - 1\}] \quad (44)$$

The nature of the critical point is indicated by the sign of Ω^2 . For $\Omega^2 < 0$, the point is of saddle type, while $\Omega^2 > 0$ indicates a centre type point. The configuration most relevant to our study is of saddle-centre-saddle type, as will be extolled upon later. This indicates a crossing of signs in the multi-critical 3-root zone of Ω^2 space should be obtained, which is exactly what follows in the results.

3.1.2 Disc in Conical Equilibrium

As before, [8]

$$\frac{du}{dr} = \frac{c_s^2 \left[\frac{2}{r} + \frac{1}{r^2(1-2/r)} \right] - f_2(r, \lambda)}{\frac{u(c_s^2 - 1)}{(1 - u^2)} - \frac{c_s^2}{u}} \quad (45)$$

The parametrised autonomous system in the $u^2 - r$ plane becomes

$$\frac{du^2}{d\tau} = 2c_s^2f_1(r) - 2f_2(r, \lambda) \quad (46)$$

$$\frac{dr}{d\tau} = \frac{1 - c_s^2}{1 - u^2} - \frac{c_s^2}{u^2} \quad (47)$$

where $f_1(r) = \frac{2}{r} + \frac{1}{r^2(1-2/r)}$

Evidently, the critical point conditions again come out to be

$$[u = c_s]_{r_c} \quad c_s = \sqrt{\frac{f_2}{\frac{2}{r_c} + \frac{1}{r_c^2(1-2/r_c)}}} \quad (48)$$

Finally, the linearly perturbed coupled dynamical system becomes

$$\frac{d(\delta u^2)}{d\tau} = -2f_1q(\gamma - 1 - c_{sc}^2)\delta u^2 + [2c_{sc}^2f'_1 - 2f'_2 - 2f_1p(\gamma - 1 - c_{sc}^2)]\delta r \quad (49)$$

$$\frac{d(\delta r)}{d\tau} = [(\gamma - 1 - c_{sc}^2)q + 1] \left[\frac{1}{u_c^2} + \frac{1}{(1 - u_c^2)} \right] \delta u^2 + (\gamma - 1 - c_{sc}^2) \left[\frac{1}{u_c^2} + \frac{1}{(1 - u_c^2)} \right] p \delta r \quad (50)$$

giving the eigenvalues

$$\Omega^2 = \frac{2}{u_c^2(u_c^2 - 1)} [f_1 p(1 + c_{sc}^2 - \gamma) + (f_2' - c_{sc}^2 f_1') \{q(1 + c_{sc}^2 - \gamma) - 1\}] \quad (51)$$

3.1.3 Flow in Vertical Equilibrium

From before, the space gradient of advective velocity is [8]

$$\frac{du}{dr} = \frac{2 \frac{c_s^2}{\gamma+1} f_1(r, \lambda) - f_2(r, \lambda)}{\frac{u}{1-u^2} - \frac{2c_s^2}{u(\gamma+1)}} \quad (52)$$

where $f_1(r, \lambda) = \frac{2}{r} + \frac{\lambda^2}{r^3} \left[\frac{1-3/r}{1-\frac{\lambda^2}{r^2}(1-2/r)} \right]$

Defining $\beta^2 = \frac{2}{\gamma+1}$ and parametrising,

$$\frac{du^2}{d\tau} = 2\beta^2 c_{sc}^2 f_1 - 2f_2 \quad (53)$$

$$\frac{dr}{d\tau} = \frac{1}{1-u_c^2} - \frac{\beta^2 c_{sc}^2}{u_c^2} \quad (54)$$

which again deliver the critical point conditions

$$u_c = \sqrt{\frac{1}{1 + \frac{1}{\beta^2 c_{sc}^2}}} = \sqrt{\frac{f_1}{f_1 + f_2}} \quad (55)$$

giving the linearly perturbed coupled dynamical system about the critical points

$$\frac{d(\delta u^2)}{d\tau} = -2(\gamma - 1 - c_{sc}^2)\beta^2 f_1 q \delta u^2 + [2\beta^2 c_{sc}^2 f_1' - 2f_2' - 2(\gamma - 1 - c_{sc}^2)\beta^2 f_1 p] \delta r \quad (56)$$

$$\frac{d(\delta r)}{d\tau} = \left[\frac{1}{(1-u_c^2)^2} + \frac{\beta^2 c_{sc}^2}{u_c^4} + \frac{\beta^2 q(\gamma - 1 - c_{sc}^2)}{u_c^2} \right] \delta u^2 + \frac{p\beta^2(\gamma - 1 - c_{sc}^2)}{u_c^2} \delta r \quad (57)$$

$$(58)$$

Thereafter, the eigenvalues come out to be :

$$\Omega^2 = -2f_1 p q \beta^4 \frac{(\gamma - 1 - c_{sc}^2)^2}{u_c^2} - \left[\frac{1}{(1-u_c^2)^2} + \frac{\beta^2 c_{sc}^2}{u_c^4} + \frac{\beta^2 q(\gamma - 1 - c_{sc}^2)}{u_c^2} \right] [2f_1 p \beta^2 (1 + c_s^2 - \gamma) + 2c_{sc}^2 \beta^2 f_1' - 2f_2'] \quad (59)$$

3.2 Isothermal Accretion

The conserved first integral of motion for isothermal accretion is [8]

$$\xi = \frac{r^2(r-2)}{[r^3 - (r-2)\lambda^2](1-u^2)} \rho^{2c_s^2} \quad (60)$$

which gives the space gradient of density

$$\frac{1}{\rho} \frac{d\rho}{dr} = \left\{ \frac{3r^2 - \lambda^2}{[r^3 - (r-2)\lambda^2]} - \frac{1}{(1-u^2)} \frac{du^2}{dr} - \frac{1}{(r-2)} - \frac{2}{r} \right\} \frac{1}{2c_s^2} \quad (61)$$

Note must be made here that now the sound speed is a global constant over space, hence plays no part in the variation.

3.2.1 Constant Height Model

For constant height model, the constant mass accretion rate is

$$\dot{M} = \frac{\rho u \sqrt{1-2/r}}{\sqrt{1-u^2}} r H \quad (62)$$

Further differentiation of \dot{M} gives a second relation for space gradient of density which on combining with (61) and parametrising in the independent parameter τ , gives the following autonomous dynamical system

$$\frac{du^2}{d\tau} = u^2(1-u^2) \left[\frac{3r^2 - \lambda^2}{r^3 - (r-2)\lambda^2} - \frac{1}{r-2} - \frac{2}{r} + 2c_s^2 \left\{ \frac{1}{r} + \frac{1}{r^2(1-2/r)} \right\} \right] \quad (63)$$

$$\frac{dr}{d\tau} = [c_s^2 - u^2] \quad (64)$$

Here again, from above, at critical point,

$$[u = c_s]_{r_c} \quad (65)$$

Now the linear perturbation scheme

$$u^2 = u_c^2 + \delta u^2$$

$$r = r_c + \delta r$$

is applied about the critical points, to obtain the following coupled system

$$\begin{aligned} \frac{d(\delta u^2)}{d\tau} = & (1 - c_{sc}^2) c_{sc}^2 \left[\left\{ \frac{6r_c}{[r_c^3 - (r_c - 2)\lambda^2]} - \frac{(3r_c^2 - \lambda^2)^2}{[r_c^3 - (r_c - 2)\lambda^2]^2} + \frac{1}{(r_c - 2)^2} + \frac{2}{r_c^2} \right\} \right. \\ & \left. - 2c_{sc}^2 \left\{ \frac{1}{r_c^2} + \frac{1}{(r_c^2 - 2r_c)^2} \right\} \right] \delta r \end{aligned} \quad (66)$$

$$\frac{d(\delta r)}{d\tau} = -\delta u^2 \quad (67)$$

The eigenvalues for this system come out to be

$$\begin{aligned} \Omega^2 = & -(1 - c_{sc}^2) c_{sc}^2 \left[\left\{ \frac{6r_c}{[r_c^3 - (r_c - 2)\lambda^2]} - \frac{(3r_c^2 - \lambda^2)^2}{[r_c^3 - (r_c - 2)\lambda^2]^2} + \frac{1}{(r_c - 2)^2} + \frac{2}{r_c^2} \right\} \right. \\ & \left. - 2c_{sc}^2 \left\{ \frac{1}{r_c^2} + \frac{1}{(r_c^2 - 2r_c)^2} \right\} \right] \end{aligned} \quad (68)$$

3.2.2 Disc in Conical Equilibrium

For mass accretion rate $\dot{M} = \Lambda \rho u \sqrt{\frac{1-2/r}{1-u^2}} r^2$ ($\Lambda = \text{const.}$) and identical treatment of the above section,

$$\frac{du^2}{d\tau} = u^2(1-u^2) \left[\frac{(3r^2 - \lambda^2)}{[r^3 - (r-2)\lambda^2]} - \frac{1}{(r-2)} - \frac{2}{r} + 2c_s^2 \left\{ \frac{2}{r} + \frac{1}{r(r-2)} \right\} \right] \quad (69)$$

$$\frac{dr}{d\tau} = c_s^2 - u^2 \quad (70)$$

Again, $[u = c_s]_{r_c}$

And linear perturbation gives

$$\begin{aligned} \frac{d(\delta u^2)}{d\tau} = (1 - c_{sc}^2)c_{sc}^2 & \left[\left(\frac{6r_c}{[r_c^3 - (r_c - 2)\lambda^2]} - \frac{(3r_c^2 - \lambda^2)^2}{[r_c^3 - (r_c - 2)\lambda^2]^2} + \frac{1}{(r_c - 2)^2} + \frac{2}{r_c^2} \right) \right. \\ & \left. - 2c_{sc}^2 \left(\frac{2}{r_c^2} + \frac{1}{(r_c^2 - 2r_c)^2} \right) \right] \delta r \end{aligned} \quad (71)$$

$$\frac{d(\delta r)}{d\tau} = -du^2 \quad (72)$$

delivering the eigenvalues

$$\begin{aligned} \Omega^2 = -(1 - c_{sc}^2)c_{sc}^2 & \left[\left(\frac{6r_c}{[r_c^3 - (r_c - 2)\lambda^2]} - \frac{(3r_c^2 - \lambda^2)^2}{[r_c^3 - (r_c - 2)\lambda^2]^2} + \frac{1}{(r_c - 2)^2} + \frac{2}{r_c^2} \right) \right. \\ & \left. - 2c_{sc}^2 \left(\frac{2}{r_c^2} + \frac{1}{(r_c^2 - 2r_c)^2} \right) \right] \end{aligned} \quad (73)$$

3.2.3 Disc in Vertical Equilibrium

For a disc in vertical equilibrium, mass accretion rate is given by

$$\dot{M} = \rho r^2 u c_s \sqrt{2[r^3 - (r - 2)\lambda^2]} \quad (74)$$

which along with ξ , gives the following autonomous system of equations in the $u^2 - r$ plane

$$\frac{du^2}{d\tau} = \left[-\frac{(3r^2 - \lambda^2)(c_s^2 + 1)}{[r^3 - (r - 2)\lambda^2]} + \frac{1}{(r - 2)} + \frac{2}{r} - \frac{4c_s^2}{r} \right] u^2(1 - u^2) \quad (75)$$

$$\frac{dr}{d\tau} = [-u^2 + c_s^2(1 - u^2)] \quad (76)$$

The critical point condition emerging from above is

$$\left[u^2 = \frac{c_s^2}{1 + c_s^2} \right]_{r_c} \quad (77)$$

Linear perturbation of the system gives

$$\frac{d(\delta u^2)}{d\tau} = u_c^2(1 - u_c^2) \left[-\frac{6r_c(1 + c_{sc}^2)}{[r_c^3 - (r_c - 2)\lambda^2]} + \frac{(3r_c^2 - \lambda^2)(1 + c_{sc}^2)}{[r_c^3 - (r_c - 2)\lambda^2]^2} - \frac{1}{(r_c - 2)^2} - \frac{2}{r_c^2} + \frac{4c_{sc}^2}{r_c^2} \right] \delta r \quad (78)$$

$$\frac{d(\delta r)}{d\tau} = -(1 + c_{sc}^2)\delta u^2 \quad (79)$$

which delivers the eigenvalues

$$\Omega^2 = u_c^2(1 - u_c^2)(1 + c_{sc}^2) \left[-\frac{6r_c(1 + c_{sc}^2)}{[r_c^3 - (r_c - 2)\lambda^2]} + \frac{(3r_c^2 - \lambda^2)(1 + c_{sc}^2)}{[r_c^3 - (r_c - 2)\lambda^2]^2} - \frac{1}{(r_c - 2)^2} - \frac{2}{r_c^2} + \frac{4c_{sc}^2}{r_c^2} \right] \quad (80)$$

4 Results And Discussion

4.1 A: The Parameter Space Dependence Of Stationary State Solutions

Figures [1a] to [2c] show the dependence of stationary state flow solutions on the flow parameters λ, ε (for polytropic), and T (for isothermal). Figures 1a,2a correspond to constant height model, 1b,2b correspond to conical equilibrium model and 1c,2c correspond to vertical equilibrium model. γ has been kept fixed at $4/3$. The dependence has been shown for all three flow geometries. For the isothermal graphs, temperature T has been scaled in units of $10^{10} K$. This parameter space classification naturally emerges as a by-result of the location of critical flow points which was necessary for this study, and has been shown here for reasons of completeness. It has also been explored in previous works, for the general relativistic case [8, 3].

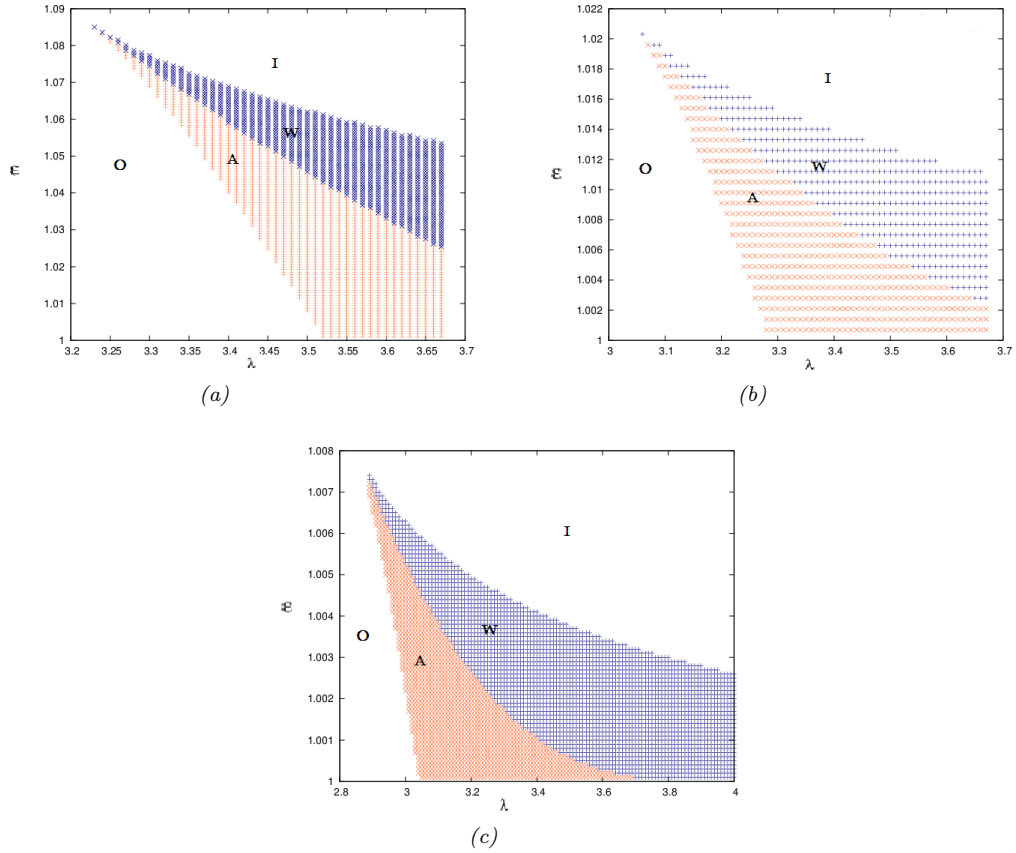


Figure 1. Parameter space for Polytropic Case

The regions O and I flanking the wedge shaped region correspond to zones where single critical points arise. These two zones occur in the two extreme regimes of low ε/T and λ , and high ε/T and λ . The physics behind them correspond to two different scenarios.

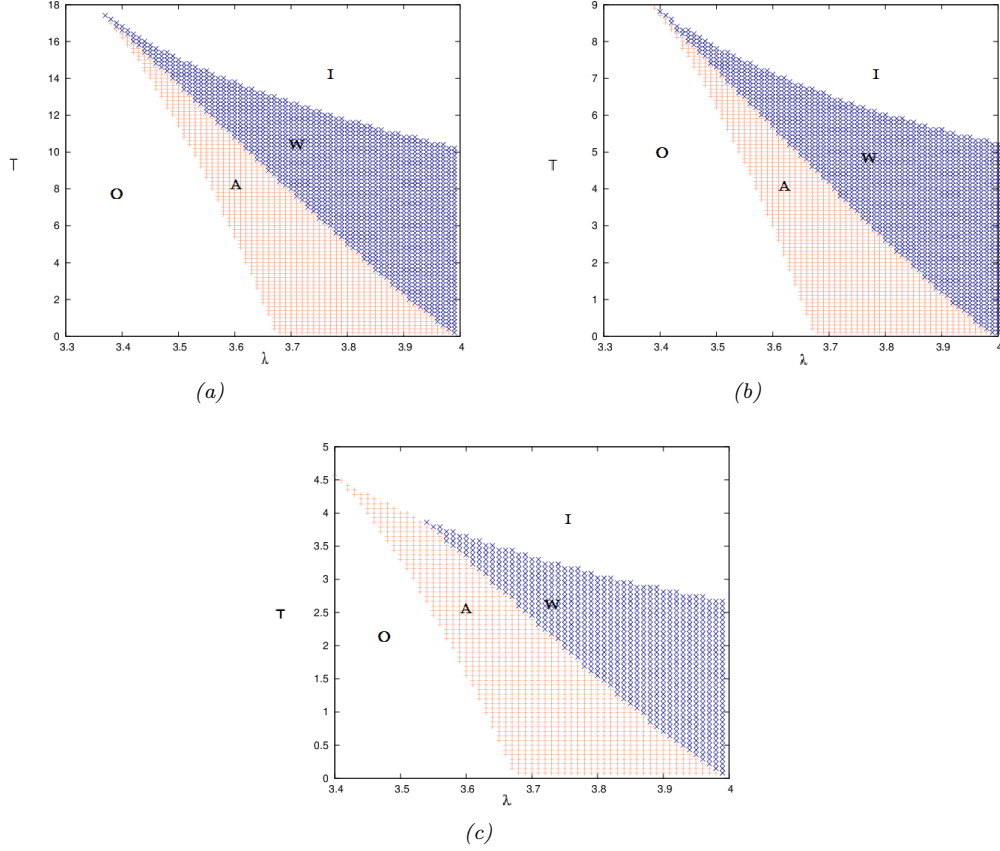


Figure 2. Parameter Space for Isothermal Case

Region O (standing for 'Outer') represents the region where the lone critical point is formed at very large distances from the event horizon. This is the case of low ε/T and low angular momentum, or 'cold flow'. The physical picture is easy to grasp. The flow starts out from the matter source very large length scales, towards the accretor (black hole), driven by its gravitational field. Unlike the case of spherical Bondi flow[18], the growth of the advective velocity field will not be monotonically growing for axisymmetric rotating accretion flow. The angular momentum sets up a centrifugal barrier that must be overcome at the cost of gravity. For this 'O' region, the λ values are very low, and weak enough for the gravity field to be able to overcome it soon enough and the flow to achieve criticality quite early on in its trajectory, when it is still far from the event horizon. The picture would be more intuitively obvious if the phase plots were explicitly obtained by numerical integration. However that has not been done, keeping in mind that the objective of this study is a dynamical systems study of the critical points.

A complete reversal of the above conditions corresponds to the region I, the erstwhile 'Inner' region or the region of 'hot' flow. Here the single critical point is formed very close to the event horizon. λ is now quite high, and comparatively so is ε/T . The accreting matter now needs to travel a large distance before the gravity field becomes sufficiently strong to overcome the resistance put up by λ and the advective velocity can catch up with the sonic velocity.

The wedge shaped region in the middle is the most striking non-trivial feature of this flow. It is the region of multicriticality, corresponding to zones where multiple critical points (namely, three) arise. It should perhaps be noted at this point that multicriticality must not automatically be taken to guarantee multitransonicity, unless some mechanism like shock transitions are possible and accessible to the system. A true multi-transonic solution can only be realised for shock solutions, if the criteria for energy preserving relativistic Rankine-Hugoniot shock for polytropic

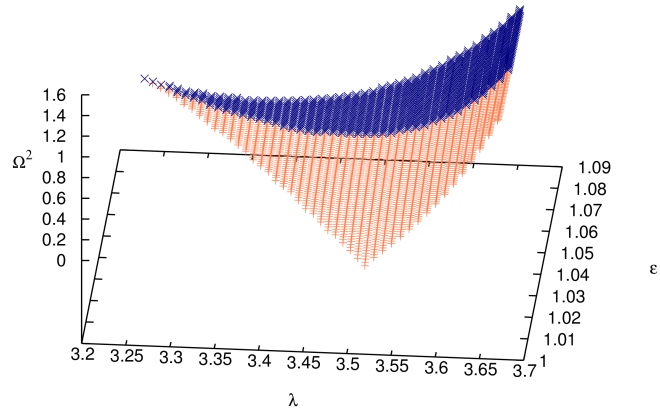
accretion and temperature-preserving relativistic shock for isothermal accretion are met [8]. As it has emerged from the results of the next section, the configuration of these three critical points is of the saddle-centre-saddle type, which is as to be expected for real, physical transonic solutions. This region has been further divided into regions marked A (accretion) and W (wind). The mathematical basis for this separation, as has already been stated earlier, is the entropy accretion rate $\dot{\Xi}$. The region A corresponds to regions where $\dot{\Xi}_{in} > \dot{\Xi}_{out}$. The wind zone is for regions with $\dot{\Xi}_{in} < \dot{\Xi}_{out}$.

From a dynamical systems point of view, the saddle-centre-saddle configuration for real, physical transonic solutions connecting infinity with the event horizon will correspond to homoclinic phase paths, on which the trajectory can double up on itself. The boundary zone between the accretion and wind zones is where the degeneracy $\dot{\Xi}_{in} = \dot{\Xi}_{out}$ holds. This degenerate locus corresponds to a heteroclinic path [5] which are notoriously unstable, and will blossom out into various kinds of bifurcations on the slightest tweaking of parameters [3].

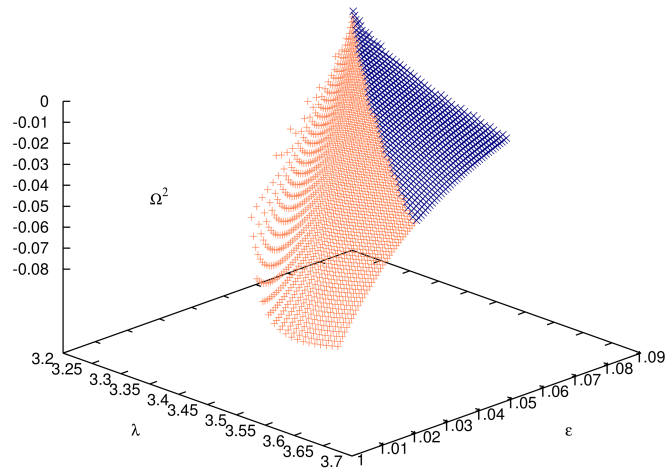
4.2 B: A Dynamical Systems Study Of The Fixed Points

The eigenvalues Ω^2 of the stability matrix corresponding to the coupled, linearized, autonomous dynamical system of the flow equations in the u^2 - r plane have been derived in earlier in Section [3], for all the three flow geometries. This has given Ω^2 as functions of the flow parameters ε/T , λ , γ , and the critical point coordinates r_c . Keeping γ fixed at $4/3$, and using the values of critical points obtained from computation of Section [2], the surface plots giving the dependence of Ω^2 on ε/T , and λ have been shown in figures [3a] to [8c]. The label [a] indicates a plot for a inner critical point, [b] for middle critical point, and [c] for outer critical point. Two different colours have been used, to indicate the accretion and wind zones (navy for wind, rust for accretion). In this section too, temperature has been scaled in units of 10^{10} .

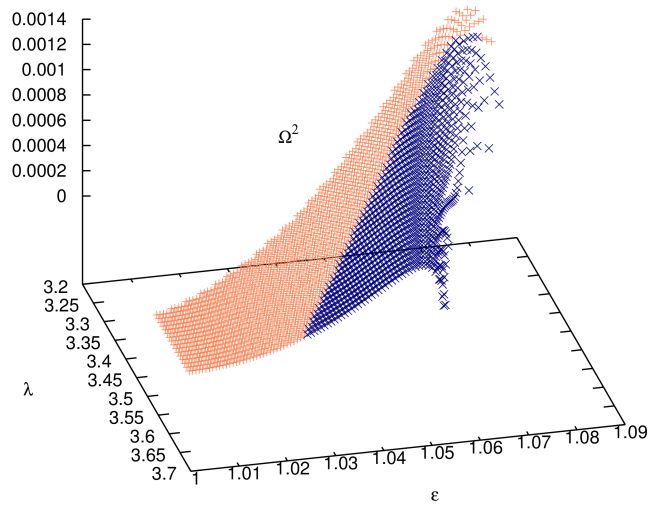
The sign of the value of Ω^2 indicates the nature of the critical point. Positive values indicate a saddle point, while negative values indicate a centre type point. It is clearly evident from the plots that the inner and outer critical points for all the flow geometries (under both polytropic and isothermal accretion) are saddle type points, flanking a centre type middle critical point. This is the only possible configuration that can allow real, physical transonic accretion flow trajectories to connect the source at infinity with the accretor via a path that can double up on itself, i.e a homoclinic path.



(a)

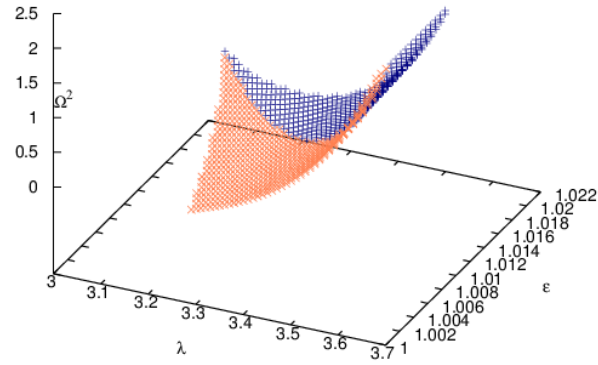


(b)

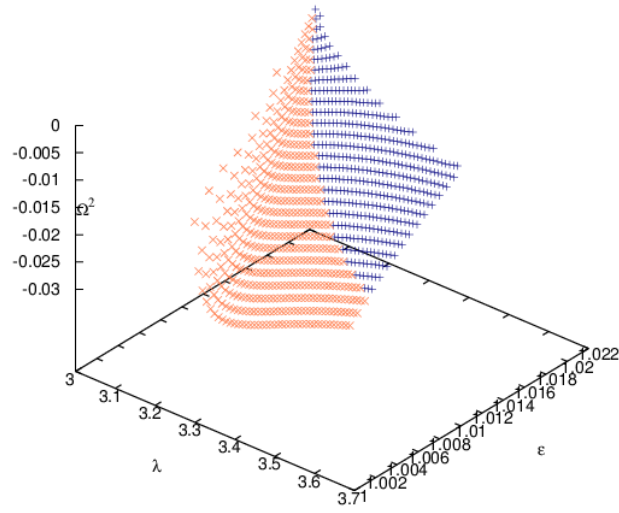


(c)

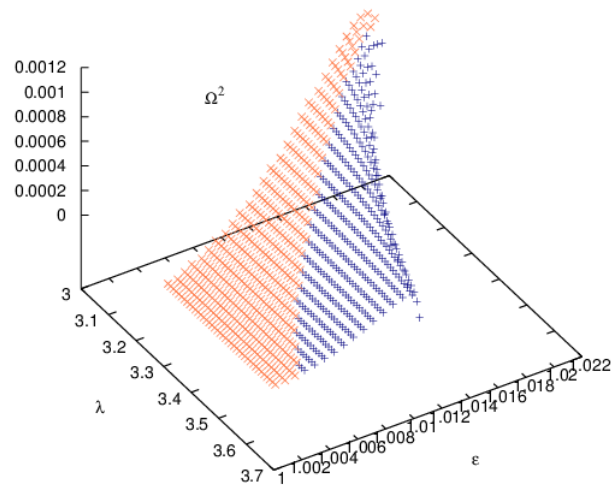
Figure 3. Constant Height for Polytropic Case



(a)

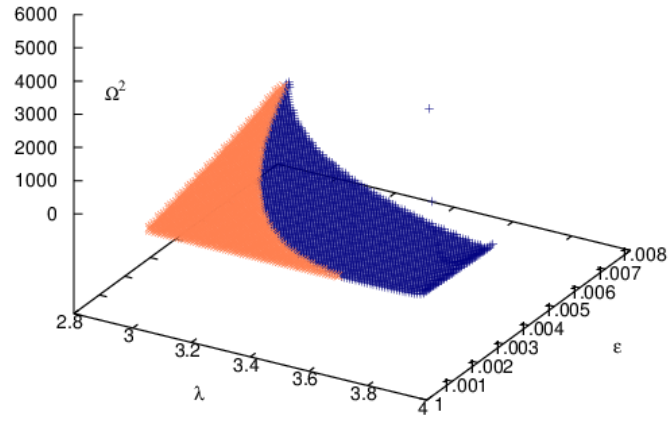


(b)

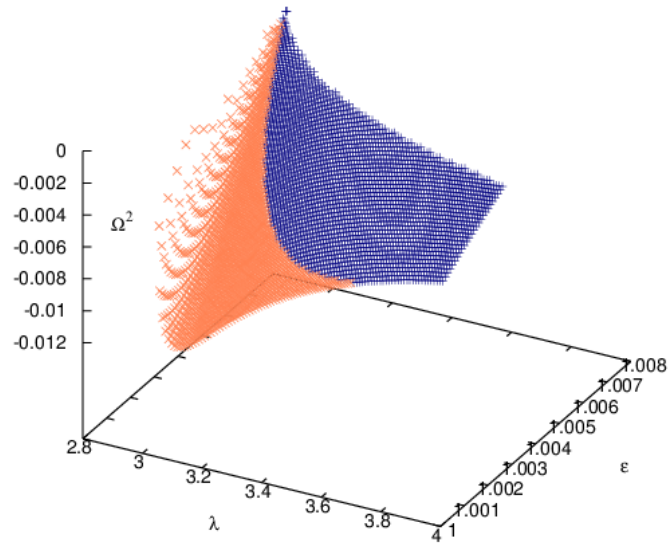


(c)

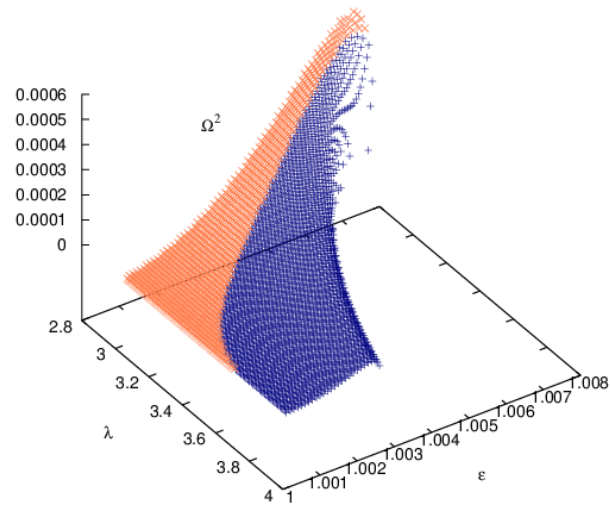
Figure 4. Conical Equilibrium for Polytropic Case



(a)

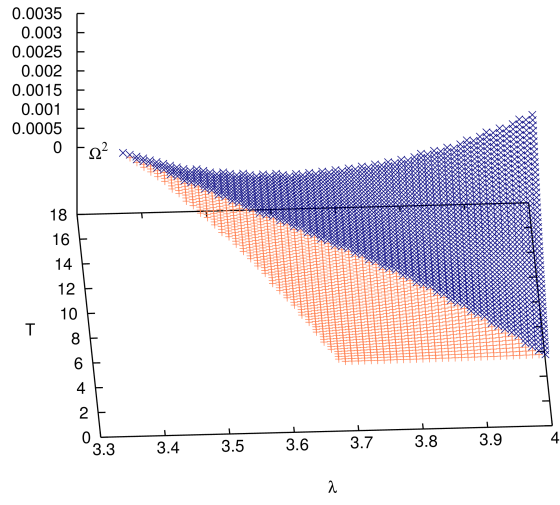


(b)

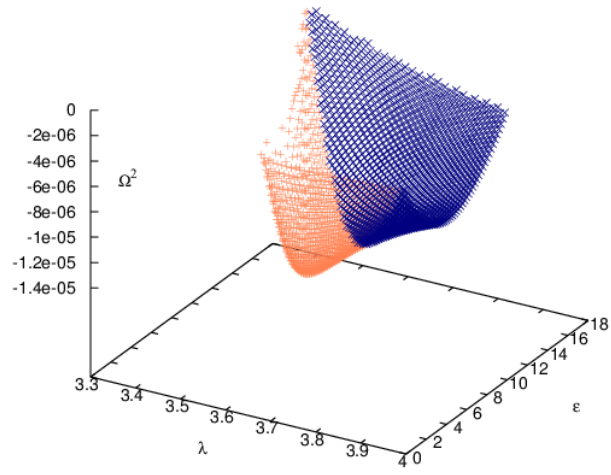


(c)

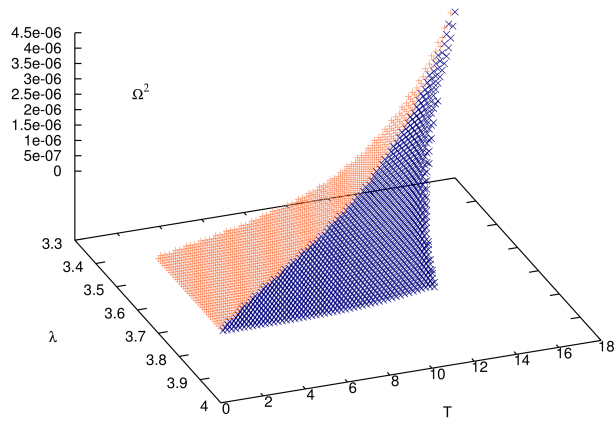
Figure 5. Vertical Equilibrium for Polytropic Case



(a)

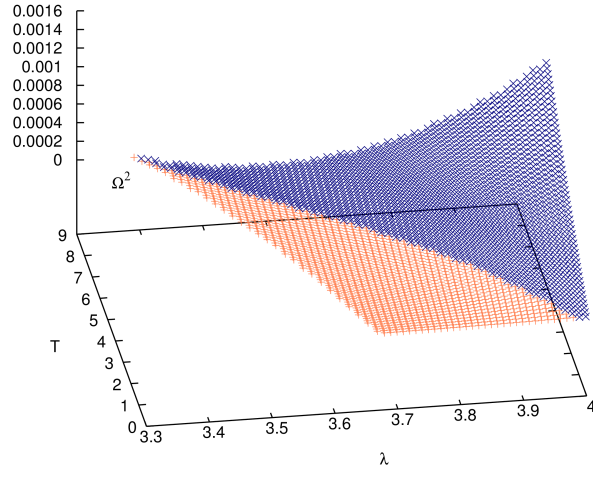


(b)

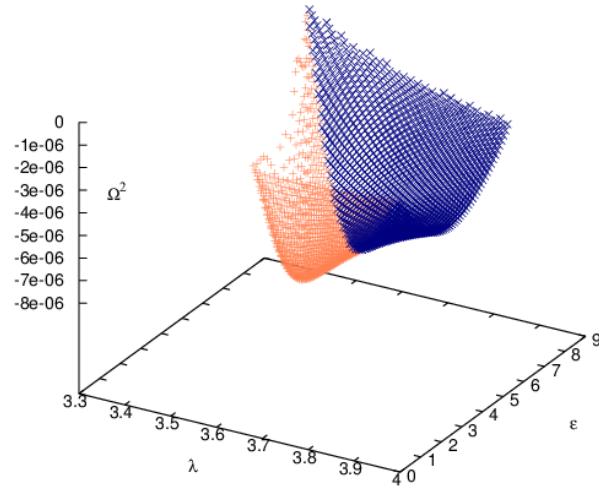


(c)

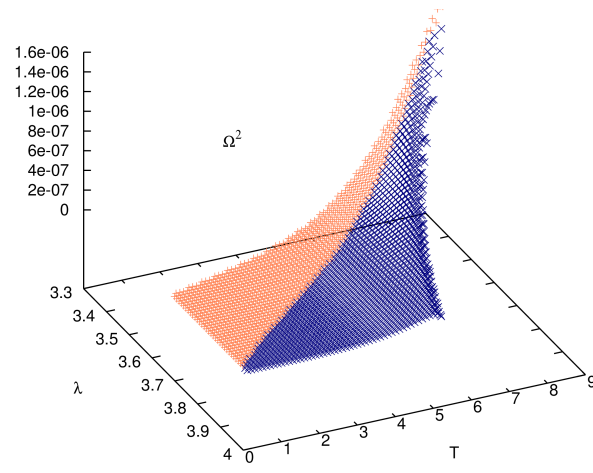
Figure 6. Constant Height for Isothermal Case



(a)

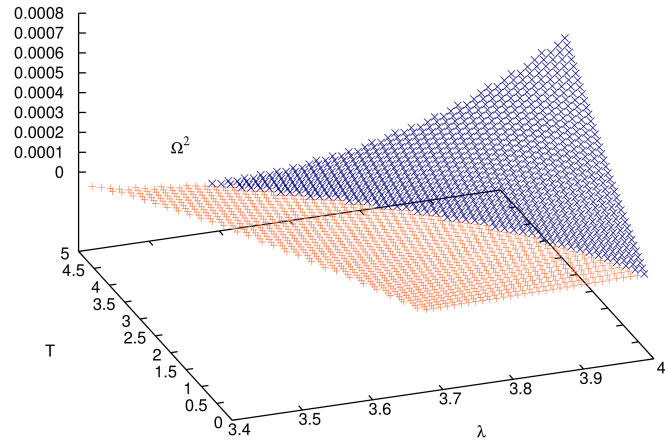


(b)

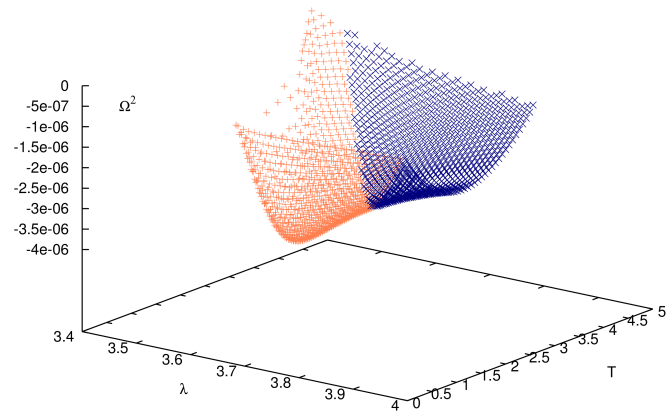


(c)

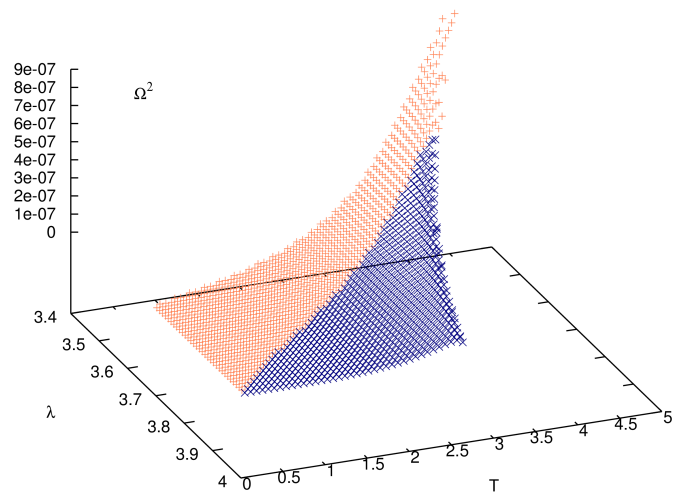
Figure 7. Conical Equilibrium for Isothermal Case



(a)



(b)



(c)

Figure 8. Vertical Equilibrium for Isothermal Case

Figures [9a] to [14b] show the projection of Ω^2 on the λ axis, now keeping ε/T also fixed along with γ . These figures make the bifurcations happening in this entire scheme more apparent. The initial region (not shown) will be that of a single critical point of saddle type, and hence Ω^2 will start out positive. At a certain value of λ , a saddle-centre type bifurcation just appears. This would correspond to a point on the junction of the O and A regions, in the parameter space. Two new critical points, a centre type and a saddle type, are born here. In Ω^2 space, they correspond to branching out of negative and positive values. As λ increases further, at a certain higher value of λ , the centre type point now coincides with one of the saddle type critical points. This merging of the centre and one of the saddle type points (the outer saddle point) corresponds to a second bifurcation in phase space. The remaining saddle point survives into the lone critical point zone. The three different branches of Ω^2 corresponding to the three different critical point coordinates, have been shown in three different colours. The branches for the middle and outer critical points (shown in green and blue respectively) are very close, but it must be noted that one lies entirely in the positive quadrant, while the other lies below. It has not been possible to resolve them further and also show all three branches on the same figure. The graphs for the accretion and wind zones have been shown on separate figures for each disc geometry, as the curves almost overlap.

A few more remarks are in order. For the surface plots, Ω^2 is seen to fall off with the critical point coordinates, as is evident from its values coming out to be largest in the plots for the inner critical point, verifying this claim. Examining the dependence on flow parameters for the two saddle type points (inner and outer), the dependence for the inner point is seen to be much weaker than the outer one. Variation of Ω^2 for the inner critical point shows very slight anti-correlated growth dependence on ε , and slow positive growth dependence on λ . Whereas for the outer critical point, variation of Ω^2 with angular momentum shows sudden, rapid rise. The change is not so marked, however, for variation with respect to flow energy ε over its entire range of variation. Another point to note is that the Ω^2 surfaces show opposite curvatures for these two cases.

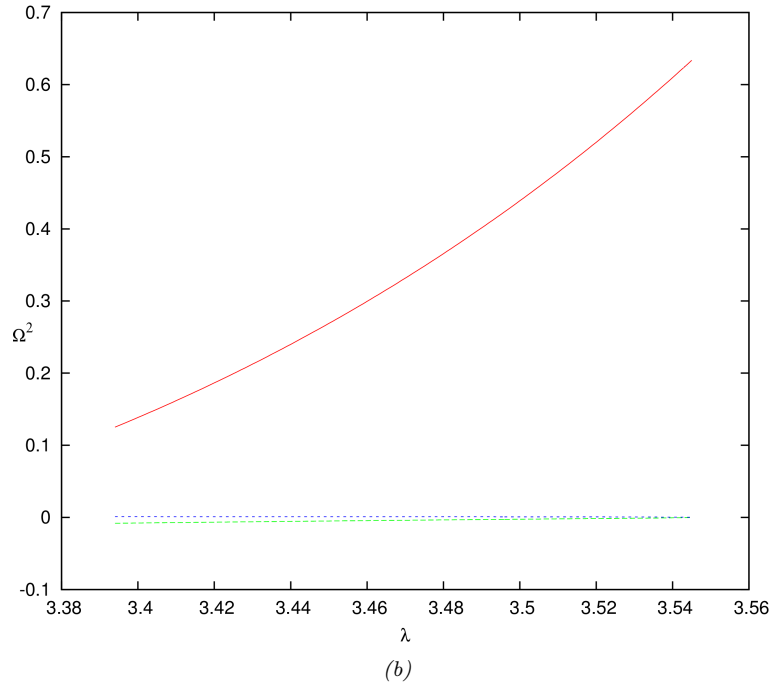
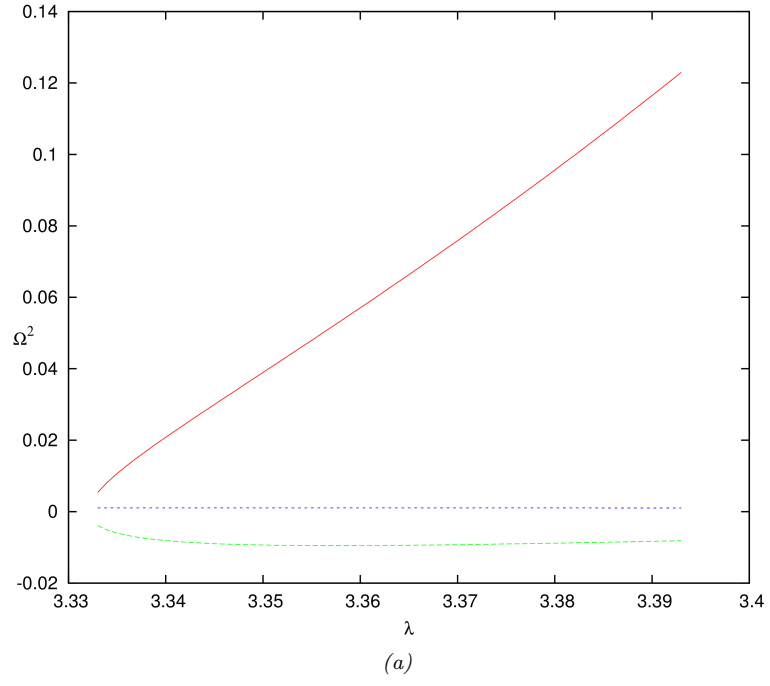


Figure 9. Constant Height for Polytropic Case

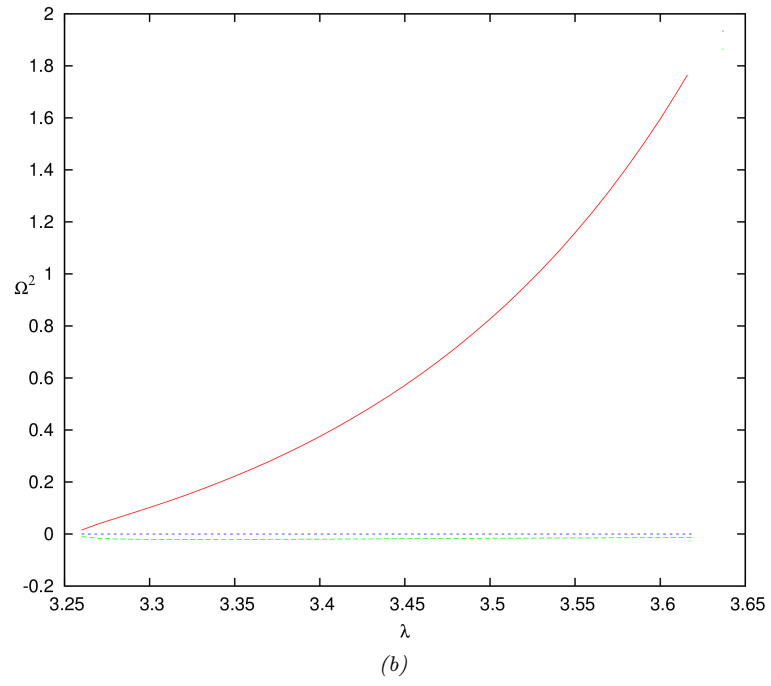
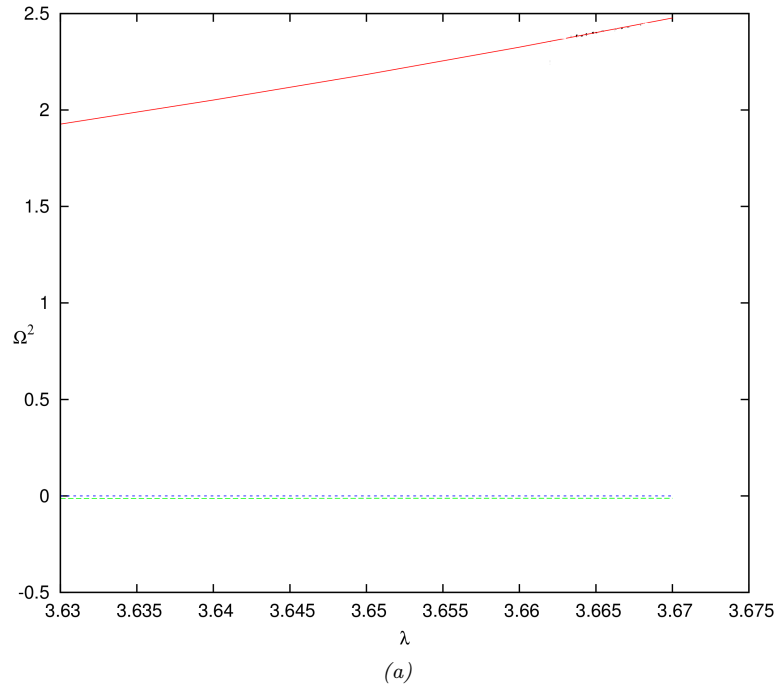


Figure 10. Conical Equilibrium for Polytropic Case

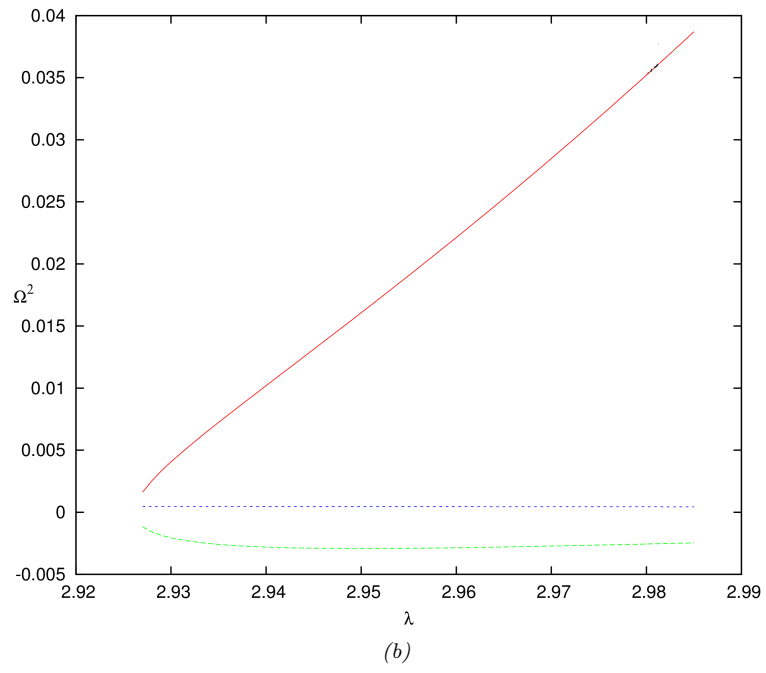
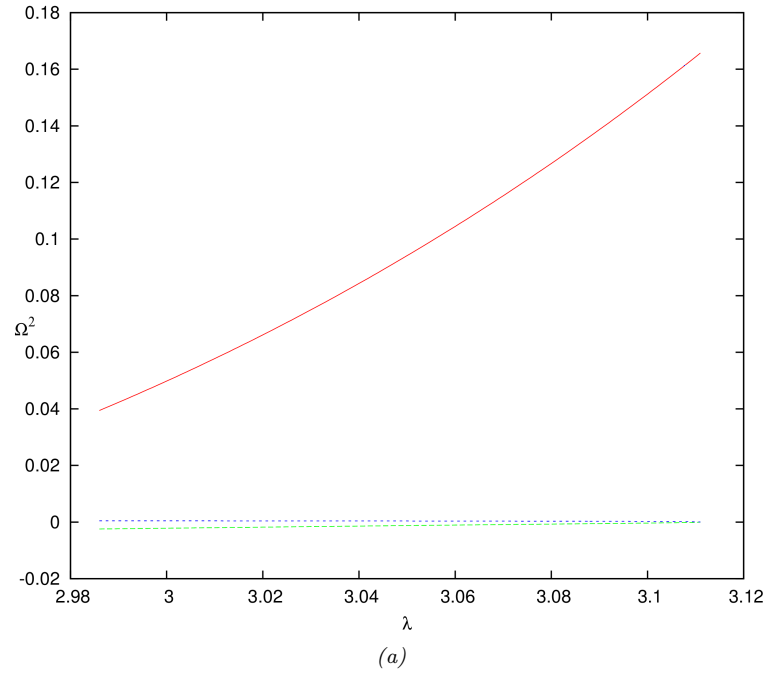


Figure 11. Vertical Equilibrium for Polytropic Case

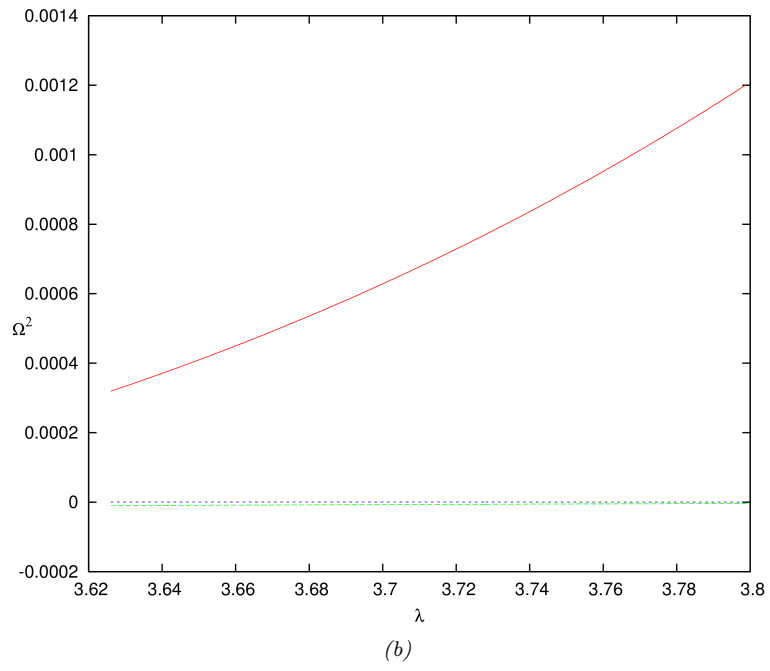
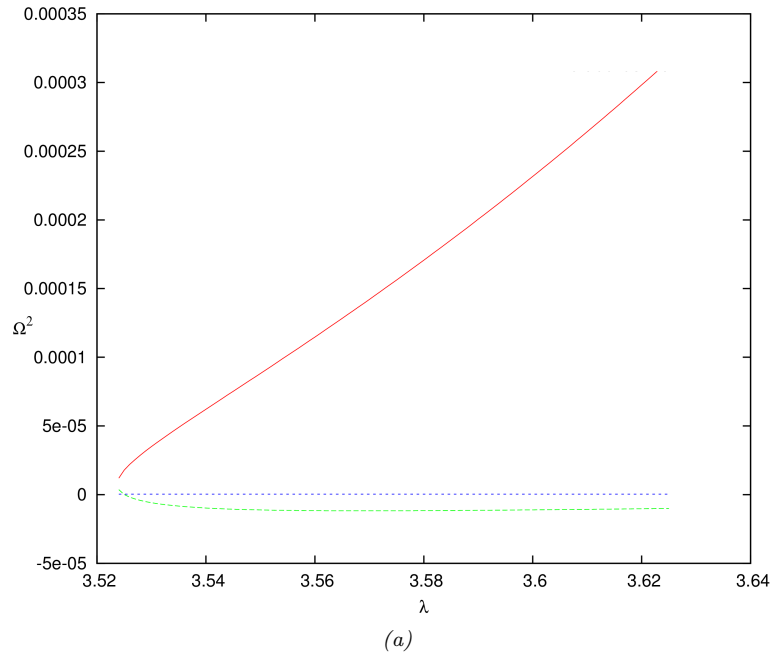


Figure 12. Constant Height for Isothermal Case

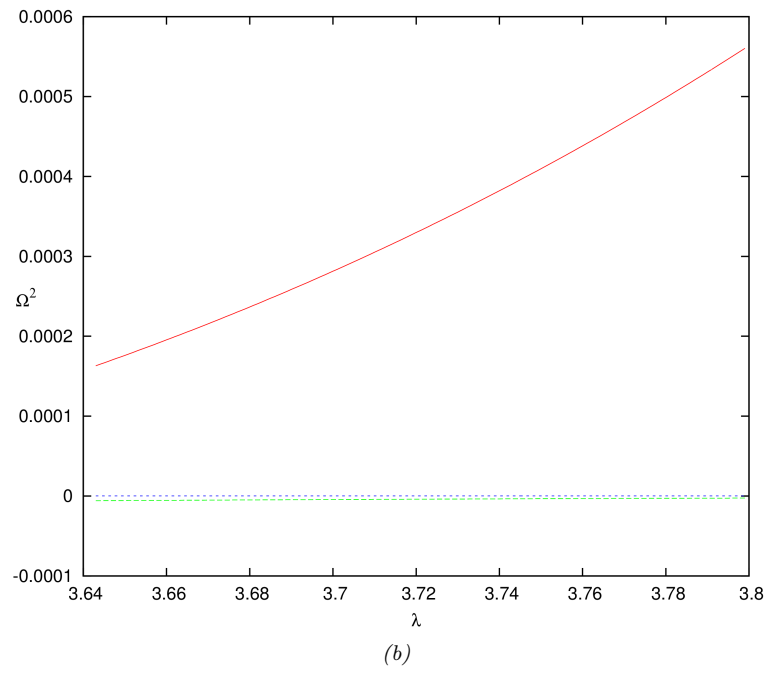
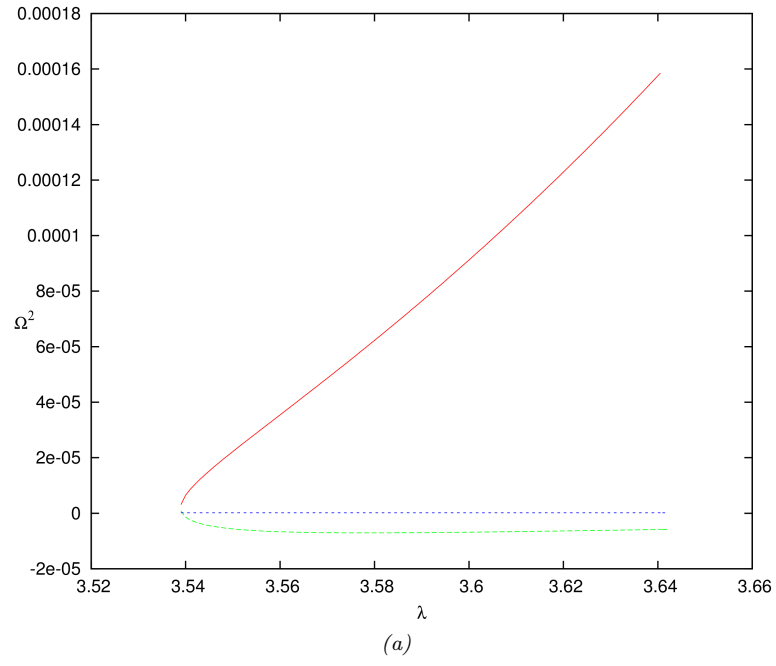


Figure 13. Conical Equilibrium for Isothermal Case

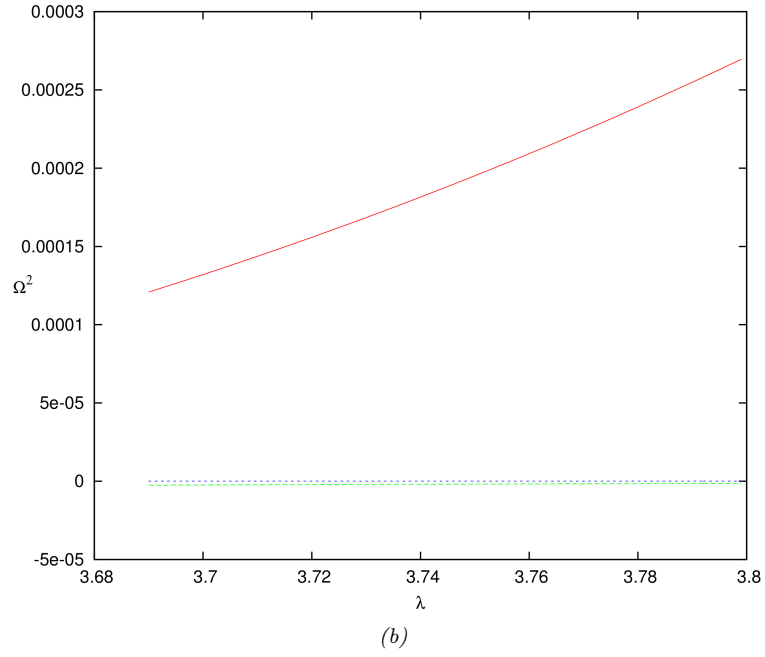
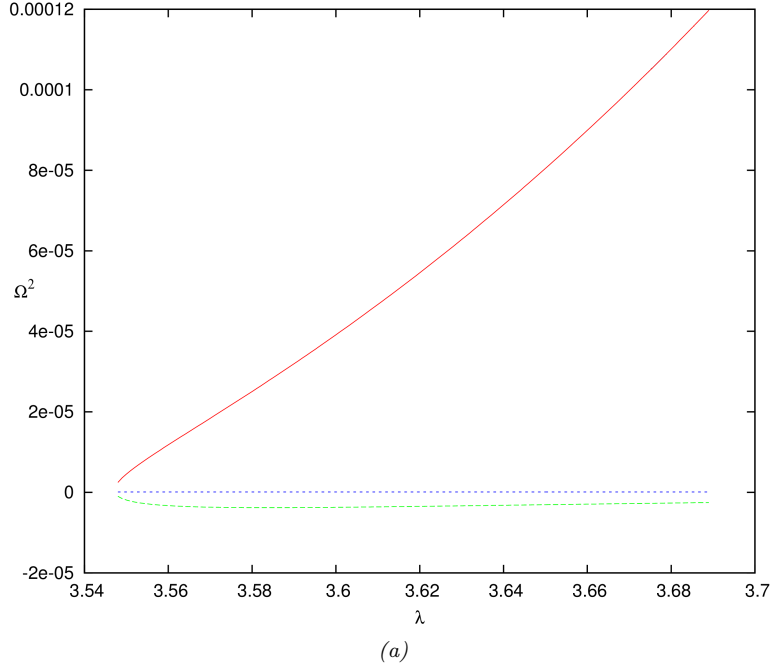


Figure 14. Vertical Equilibrium for Isothermal Case

5 Concluding Remarks

The main focus of this study was axially symmetric multi transonic accretion in strong gravity. The time independent, general relativistic fluid equations governing the accretion flow onto a Schwarzschild black hole were studied, for different geometric configurations of the accretion disc and under different thermodynamic conditions. This was done by identifying the coupled differential equations of the flow velocity and critical radial coordinate with a first order autonomous

dynamical system. Thereafter a linear variational analysis of this system was carried out around the critical points. This treatment necessitated locating the critical points, and the parameter space spanned by the initial boundary conditions could be identified. The most interesting feature that emerged from this was the multicritical zone. However axisymmetric black hole accretion is repeatedly cited as an example of multi-transonic accretion. It is reiterated here that multi-criticality must not be taken to be topologically isomorphic with multi-transonicity [8]. The possibility of shock solutions to arise in the system, must exist, where the Rankine-Hugoniot shock conditions are satisfied at the shock front. A full treatment in the general relativistic framework, for locating these shocks, and investigating the dependence of the shock location, as well as pre- to post shock ratios of various accretion variables, on different dynamical and thermodynamic properties of the flow, forms future motivation.

Further, this entire treatment has been of a stationary case. Transient phenomena form the basis for evolutionary behavior of astrophysical structures. The stability of the stationary solutions obtained is still open to exploration, as well as the relevant astrophysical time scales over which they are so. This can be achieved through the usual technique of (linear) perturbation analysis of the full dynamical fluid equations (governing the accretion flow) around the stationary solutions. The dispersion relation so obtained would give a comprehensive idea regarding the various time scales governing growth patterns of acoustic perturbation in the accretion disc, as well as the factors determining them. Further, it can be demonstrated that a relativistic acoustic geometry embedded by the background stationary space time may be obtained sustaining the propagation of these acoustic perturbations. This forms the basis for considering black hole systems as a classical analogue gravity model that could be naturally found in the universe. Most importantly, the system would demonstrate dual existence of event and acoustic horizons- a rich and unique, non trivial feature of this model. Acoustic surface gravity could hence be calculated, and related analogue Hawking temperature as well [8].

Acknowledgments

This work was the culmination of a visiting students research programme at HRI, Allahabad, and completed under the tutelage of Prof. Tapas. K. Das (Faculty, HRI). SI would like to acknowledge all the guidance, discussions with, and suggestions of Prof. Das. The discussions with Pratik Tarafdar were also found very helpful. HRI resources were made use of, and the kind hospitality provided availed during this period, and this is also duly acknowledged.

References

- [1] York, D. G., Gingerich, O., Zhang S. N. eds, 2011, *Astronomy Revolution: 400 Years of Exploring the Cosmos*, Taylor and Francis Group LLC/CRC Press
- [2] Chakrabarti, S.K., 1990, *Theory of Transonic Astrophysical Flows*, World Scientific Press, Singapore
- [3] Goswami, S., Khan, S.N., Ray, A.K., Das, T.K., 2007, *MNRAS*, 378, 1407
- [4] Chakrabarti, S.K., 1989, *ApJ*, 347, 365
- [5] Jordan, D.W., Smith, P., 1999, *Nonlinear Ordinary Differential Equations.*, Oxford Univ. Press, Oxford
- [6] Paczynski, B., Wiita, P. J, 1980, *A & A*, 88, 23
- [7] Nag, S., Acharya, S., Ray, A.K., Das, T.K., 2011, *New Astronomy*, 17, 285
- [8] Tarafdar, P., Das, T.K., 2013, *arXiv:1305.7134v3*

- [9] Illarionov, A.F., & Sunyaev, R.A., 1975a, *A & A*, 39, 205
- [10] Liang, E.P.T., Thomson, K.A., 1980, *ApJ*, 240, 271
- [11] Bisikalo, A.A., Boyarchuk, V.M., Chechetkin, V.M., Kuznetsov, O.A., Molteni, D., 1998, *MNRAS*, 300, 39
- [12] Illarionov, A.F., 1988, *Soviet Astron.*, 31, 618
- [13] Ho, L.C., 1999, in *Observational Evidence for Black Holes in the Universe*, ed. S. K. Chakrabarti (Dordrecht: Kluwer), 153
- [14] Anderson, M., 1989, *MNRAS*, 239, 19
- [15] Barai, P., Das, T.K., Wiita, P.J., 2004, *ApJ*, 613, L49
- [16] Das, T.K., Bilic, N., Dasgupta, S., 2007, *JCAP*, doi:10.1088/1475-7516/2007/06/009
- [17] Chaudhury, S., Ray, A.K., Das, T.K., 2006, *MNRAS*, 373, 146
- [18] Bondi, H., 1952, *MNRAS*, 112, 195